[Article ID] 1003 - 6326(2000)06 - 0794 - 04

Injection molding of nano-structured 90 W-7 Ni-3 Fe alloy powder prepared by high energy ball milling①

FAN Jing-lian(范景莲), QU Xuan-hui(曲选辉), HUANG Bai-yun(黄伯云)
(The State Key Laboratory for Powder Metallurgy, Central South University, Changsha 410083, P.R.China)

[Abstract] Blended elemental 90 W-7 Ni-3 Fe (mass fraction, %) powder was mechanically alloyed in a planetary ball mill. Nano-crystalline grains were obtained after 10 h milling. The nano-structured powder was processed to full density by metal injection molding approach. Compacts from the optimal powder-binder mixture were studied for molding and sintering behaviors. Milling significantly increases the maximum powder loading and homogeneity of the feedstock, and enhances the sintering densification process. When solid-state-sintered at 1 350 ~ 1 450 ℃, the alloy shows very fine grains (~3 μm), high tensile strength (>1 130 MPa) and almost no distortion.

[Key words] tungsten heavy alloy; nano-structured powder; injection molding
[CLC number] TF125.2; TG146.4 [Document code] A

1 INTRODUCTION

Tungsten based alloys are unique materials and have been widely used in all fields, due to their combination of high density, strength, ductility, conductivity, machinability and formability. Full densification of tungsten heavy alloys are typically produced via liquid phase sintering of 78 % ~ 98 % (mass fraction) W powder blended with the balance of Ni and Fe powders as a matrix-binder phase. Powder injection molding (PIM) is a new powder-forming process, which begins with mixing powder and binder, then the mixture is granulated and injection-molded into the desired shape. The binder in the formed compacts is removed before sintering. PIM provides an economic advantage in mass production[1,2] of tungsten heavy alloys with complex shaped parts. However, the relatively high sintering temperature and large difference in density between solid and liquid phase result in progressive slumping and distortion of the compacts during sintering[3~6]. It is obvious that if the compacts can be sintered at the temperatures below the liquids temperature the distortion may be eliminated.

Pre-alloyed powder prepared by freeze drying[7], CVD, RSP[8] and high-energy ball milling can greatly enhance sintering process. In particular, after milling, the apparent density and tapping density of the powders are increased, and the average particle size is decreased[9], which is very useful to PIM. In this study, nano-grain sized 90 W-7 Ni-3 Fe powder is prepared by high-energy ball milling. The injection molding of this nano-crystalline powder is investigated, including feedstock homogeneity, optimal powder loading and sintering behavior.

2 EXPERIMENTAL

The initial powder composition was composed of 90 % tungsten, 7 % nickel and 3 % iron powder. The metal powders were reduced tungsten, carbonyl iron and nickel powders. Their particle sizes (Fsss) are 2.91, 2.66 and 3.97 μm respectively. The mixed powders were subjected to mechanical alloying in a QM-1 planetary ball mill, in which tungsten balls were used. The mass ratio of ball to powder was 5∶1. The rotation speed of the sun disc and the jar was 200 r/min. The experiments were carried out in a high purity argon atmosphere.

Characteristics of the milled powders were analysized by X-ray diffraction and Brunaure-Emmett-Teller (BET) nitrogen adsorption technique.

After milled, the powders were mixed with a wax-based multi-component binder. The viscosity and optimal powder loading of the powder-binder mixture were measured. Then the powder binder mixture were granulated and injection-molded. The molded compacts were then thermally debinded and sintered to full density.

3 RESULTS AND DISCUSSION

3.1 Characteristics of milled powders

The characteristics of the milled powders after various times of milling are shown in Table 1. With the increase of milling time, the crystalline size greatly decreases, the lattice distortion increases and the specific surface area lightly decreases. The initial W

① [Foundation item] Project (59634120) supported by the National Natural Science Foundation of China and project (715 - 090 - 090) supported by the National Advanced New Technology Fund [Received date] 2000 - 04 - 10; [Accepted date] 2000 - 07 - 01

Table 1 Characteristics of milled powders

Milling time/ h	Crystalline size/ nm	Lattice distortion / %	Specific surface area/ ($m^2 \cdot g^{-1}$)
0	332	0.05	0.52
5	63	0.41	0.45
10	28	0.46	0.41
20	17	0.59	0.38

crystalline size is 332 nm. After 10 h of milling, the W crystalline size decreases to 28 nm. After 20 h of milling, the crystalline size refines to 17 nm.

These results indicate that the nano-crystalline size powders can be obtained after milled over 10 h. The refinement of crystalline size and the increasement of lattice distortion are resulted from high speeds of collision between powders and balls during milling process. High density of dislocations and defects are produced within particles during milling.

Specific surface area is relevant to several factors: particle size and particle size distribution, inner pores, particle shape, agglomeration and homogeneity of elemental powder distribution. The decrease of specific surface area can result in an increase of the apparent density and tapping density, which is agreed with the results in Ref.[9]. Higher apparent density and tapping density are very useful to PIM.

Fig.1 shows the morphologies of the initial W powder and the 10 h milled powders. The initial W powder shows multi-crystalline and agglomeration. Before milling, the specific surface area is higher, because many small particles collect together to form a soft agglomerated powder, in which the bonding force between particles is lower, the inner pores are higher, and the bonding interface area is lower. Compared with the initial powder, the morphology of the milled powder is more regular, similar to a spherical particle. The specific surface area decreases a little because of hard agglomeration among W, Ni, Fe powders formation. Milling results in a uniform distribution of W, Ni and Fe powders. Due to repeated collision, extrusion cold-welding and fracture between powders, the milled powders gradually lose the initial morphologies of W, Ni and Fe powders.

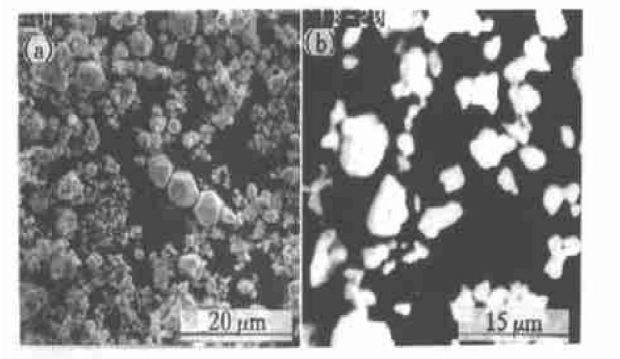

Fig.1 Morphologies of initial W powder (a) and milled powder mixture (b)

3.2 Properties of feedstock

3.2.1 Viscosity

Fig.2 shows viscosity of the feedstock variation with milling time. The viscosity decreases with milling, especially at the beginning of milling. This indicates that changes of powder characteristics have great effects on the viscosity of feedstock. The powder with higher specific surface area and more pores will require more binder to coat it, and results in lower powder loading, polymer binder can not efficiently distribute among particles, which would result in difficulties in the relative movement of particles. Milling decreases the specific surface area so that increases homogeneity of feedstock.

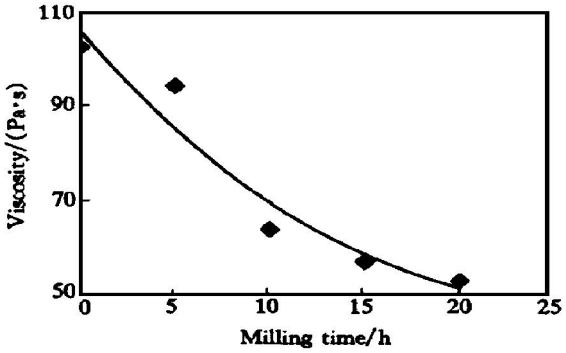

Fig.2 Variation of viscosity with milling time

3.2.2 Optimal powder loading

Fig.3 shows the relationship between powder loading and density of feedstock. With the increase of powder loading, the density of feedstock increases. Theoretically, the density linearly increases with powder loading, which is as[11]

$$\rho = \rho_b + \varphi(\rho_p - \rho_b) \quad (1)$$

where ρ_b is the theoretical density of the binder, ρ_p is the theoretical density for the powder mixture, φ is the powder volume fraction, and ρ is the theoretical density of the feedstock.

Generally, the actual density of the powder mixture is lower than its theoretical density, due to the

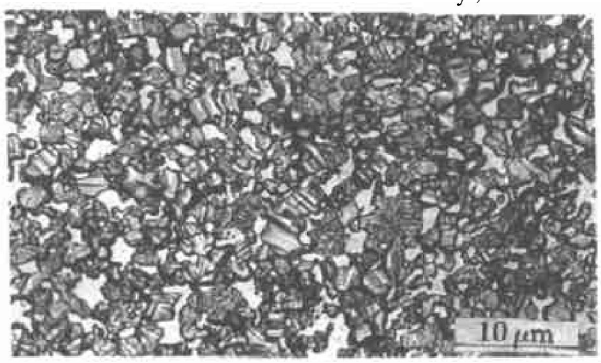

Fig.3 Relationship between powder loading and mixture density

pores inside the powders. Furthermore, during mixing of feedstock, air can be easily encapsulated into the mixture, which results in bubbles in the feedstock. Both of the two factors will lead to lower actual density of feedstock. The deviation of the actual density from the theoretical density can reflect some important information. The increase of deviation indicates that binder is insufficient to fill the spaces between the powders. Since the powder cannot flow to fill all space, voids forms in the mixture, and the binder can not uniformly blend with powder, the powder loading reaches to the critical loading. At powder concentrations over the critical loading, the mixture density will fall far below the theoretical density because of increase in voids. It is seen from Fig.3 that the critical powder loading of the un-milled powder mixture is only 0.57.

While the critical powder loading of the 10 h-milled powder mixture can reach up to 0.61, the increase of powder loading is helpful to the control of distortion.

3.3 Densification, microstructure and properties

Fig.4 illustrates the variation in density of sintered samples with sintering temperature. Milling enhances the consolidation process. Obvious densification for the un-milled powders takes place at the temperature over 1 300 ℃ and the full densification can only be obtained at the temperature over 1 500 ℃. In comparison to the un-milled powder, the densification temperature of the nano-structured powder is lowered greatly; fully densified alloy is obtained through solid-state sintering at the temperatures of only 1 350 ~ 1 450 ℃. Therefore, the slumping and distortion induced by liquid phase sintering can be completely avoided by the enhanced solid-phase sintering process.

The relationship between the active energy for densification and sintered density can be expressed as[10]

$$\ln[(\rho-\rho_0)/(1-\rho_0)] = \ln[C/(1-\rho_0)] - Q_d/(RT) \quad (2)$$

where ρ is the density of the sintered sample, ρ_0 is the density of the green part, C is a constant, R is the gas constant, and T is the sintering temperature. The active energy for densification Q_d determines densification speed.

Fig.5 shows the relationship between density and temperature. The value of Q_d can be determined from Fig.5. The values of Q_d for the un-milled and 10 h-milled powder are 119 kJ/mol and 58.4 kJ/mol respectively. Large defects, nano-crystalline, super-solidus solution and amorphous phase produced by milling are responsible for the enhanced sintering[11,12].

Fig.5 Curves of $\ln[(\rho-\rho_0)/(1-\rho_0)]$ vs $1/T$

Fig.6 shows the microstructure of the alloy sintered at 1 400 ℃. The microstructure of the fully densified alloy has very fine W grains. The W grain sizes are about 3 μm, which is one-tenth of that of the traditional liquid phase sintered alloy. The result of mechanical property shows that the solid sintered has very high tensile strength. The maximum tensile strength is 1 130 MPa, which is 200 MPa higher than that of the traditional liquid sintered alloy. Mechanical property is relevant to microstructure, including porosity and grain size. Their relationship can be expressed as[12]

$$\sigma = \sigma_0 G^{-2}\exp(-\beta\varepsilon) \quad (3)$$

Fig.4 Variation of density with sintering temperature

Fig.6 Optical microstructure of alloy sintered at 1 400 ℃

where σ is the strength, σ_0 is a constant, G is the grain size and ε is the porosity. The finer the grain size is, the higher the properties of the alloy are. Therefore, the refinement of W grain size is the real reason for the higher strength.

4 CONCLUSIONS

1) During milling, powder characteristics change greatly. Milling results in the formation of nano-crystalline powder and change of powder morphology.

2) Milling increases density of feedstock and decreases viscosity. By milling, the critical powder loading is increased.

3) Milling enhances consolidation process. Full densification of the alloy can be obtained via solid state sintering at 1 350 ~ 1 450 ℃. The slumping and distortion resulted from liquid phase sintering can be avoided completely.

4) Milling greatly increases the tensile strength due to finer W grain size of the alloy.

[REFERENCES]

[1] German R M. Powder Injection Molding [M]. Princeton: Metal Powder Industries Federation, 1990.

[2] FAN Jing-lian, HUANG Bo-yun, QU Xuan-hui, et al. Properties and microstructure of tugnsten heavy alloy by injection molding [J]. The Chinese Journal of Nonferrous Metals, (in Chinese), 1998, 8(4): 590.

[3] Heaney D F, German R M and Ahn I S. The gravity effect on critical volume fraction during liquid phase sintering [A]. Advances in Powder Metallurgy [C]. Princeton: Metal Powder Industries Federation, 1993, 2. 169.

[4] German R M. Limitations in net shaping by liquid phase sintering [A]. Advances in Powder Metallurgy [C]. Princeton: Metal Powder Industries Federation, 1991, 4. 183.

[5] YANG S C and German R M. Gravitational limit of particle volume fraction in liquid phase sintering [J]. Metall Trans A, 1991, 22A(3): 786.

[6] FAN Jing-lian, HUANG Bo-yun, QU Xuan-hui, et al. Investigation on distortion of PIM tungsten heavy alloy during liquid phase sintering [J]. Journal of Central South University of Technology, (in Chinese), 2000, 31(10): 47 - 50.

[7] White G D and Gurwell W D. Freezed-dried tungsten heavy alloys [A]. Advances in Powder Metallurgy [C]. Princeton: Metal Powder Industries Federation, 1989, 1: 355.

[8] Sylvia T F, Thomas H and Theodor S. Taylor-made tungsten heavy alloys by solid state sintering of pre-alloyed powders and subsequent add working [A]. Tungsten Refract Met-1994, Proc Int Conf [C]. Princeton: Metal Powder Industries Federation, 1995, 2. 169.

[9] Belhadjhamida A and German R M. The effects of powder pretreatment on the microstructure and mechanical properties of tungsten heavy alloy [A]. Advances in Powder Metallurgy [C]. Princeton: Metal Powder Industries Federation, 1991, 6: 407.

[10] Johnson J L and German R M. Chemically activated liquid phase sintering of tungsten-copper [J]. Int J of Powder Metall, 1994, 30(1): 91.

[11] FAN Jing-lian, HUANG Bo-yun, QU Xuan-hui, et al. W-Ni-Fe nano-structure materials synthesized by high energy ball milling [J]. Trans of Nonferrous Met Soc China, 2000, 10(1): 57.

[12] Aning A O, Whang Z and Courtney T H. Tungsten solution kinetics and amorphization of nickel in mechanically alloyed Ni-W alloys [J]. Acta Metall Mater, 1993, 41(1): 165.

(Edited by LONG Huai-zhong)